Microscopic Density Functional Theory for Dendrimers

Alexandr Malijevský*
Department of Chemical Engineering, Imperial College London, South Kensington Campus, London SW7 2AZ, United Kingdom and E. Hála Laboratory of Thermodynamics, Institute of Chemical Process Fundamentals of the ASCR, 165 02 Prague 6, Czech Republic
(Dated: November 12, 2012)

Density functional theory for a simple model of dendrimers is proposed. The theory is based on fundamental measure theory which accounts for the hard-sphere repulsion of the segments and on the Wertheim first-order perturbation theory for the correlations due to connectivity. Set of the recurrence formulae for the ideal chain contribution involving simple integrals is derived. By using perturbation theory dispersion forces can be easily included.

Dendrimers (also known as arborols or cascade molecules) are repeatedly branched monodisperse compounds with a fractal-like structure possessing a high degree of symmetry. The first dendritic structure was constructed by Vögtle et al. in 1978 [1] using a repetitive synthesis strategy (divergent synthesis) such that one new molecular layer (generation) is created in each reaction cycle. Almost immediately dendrimers attracted increasing attention due to their unique structure implying some unique properties compared to traditional linear chains. With increasing number of generations the number of chain-ends increases exponentially and that is why dendrimers adopt a compact globular shape. As a consequence the dendrimers' solubility is driven by the nature of surface groups only [2]. Moreover, the presence of internal cavities enables encapsulation of small guest molecules [3]. Such properties predestinate dendrimers for a variety of possible technological application. They are being developed for use in fields such as catalysis, magnetic resonance imaging, drug delivery, coatings, electronics or cancer therapy [4–7].

In terms of theoretical study and in particular of physical model used, there are in principle two perspectives in treating such complex structures. First, one can use so-called coarse graining technique treating molecules as spherically symmetric objects interacting via some effective soft potential, i.e. the degrees of freedom of monomers composing the polymer are integrated out. Perhaps the first who proposed such a strategy was Flory [8], but it has become popular only in recent times [9, 10]. The coarse-grained approach was applied for dendrimers by Götze et. al [11] who approximated the interaction between two dendrimers in solution by an appropriate Gaussian function. Even though the coarse-graining method is attractive in simplifying the description of a given complex structure substantially, it inevitably loses some information about the intrinsic property of the molecules. Moreover, the radial symmetry of an effective potential is more justified in a bulk phase rather than e.g. in the vicinity of a wall. For these reasons, a second approach, treating the complex molecular systems on an atomistic level, would seem to be to superior. Microscopic density functional (DF) theory provides a versatile and powerful tool to represent the microscopic structures and interfacial phenomena of polyatomic fluids under a variety of situations. Woodward developed a theory that combines weighted density approximation, known from theories of simple fluids, with single-chain Monte Carlo simulations [12]. An alternative DFT of inhomogeneous polymer solutions was formulated by Forsman et al. [13]. Their theory is based on the free energy functional resulting from the generalized Flory equation of state. However, an approach due to Yu and Wu [14] which incorporates Wertheim's perturbation theory for a bulk fluid [15, 16] into the non-local DF framework proposed by Rosenfeld [17] revealed to be particularly appealing. In the spirit of the Rosenfeld fundamental measure theory (FMT), Yu and Wu constructed a non-local functional accounting for the chain connectivity. Such an approach has proved to be both quantitatively accurate and computationally convenient and eventually has been extended for a variety of models of e.g. cyclic polyatomic fluids [18], block copolymers [19], star polymers [20], polydisperse polymers [21] or for brush-like structures [22]. Recently, a so-called hybrid approach for the structure of dendrimers has been proposed [23] in the spirit of Ref. [12]. In this paper, a full density functional is derived and used to represent hard dendrimers confined between two hard walls.

In the following, by the term "dendrimer" will be taken to mean the special case of a tree structure where each segment apart from the terminating ones has the same number of bonds, three at minimum. Due to the high level of symmetry the system can be characterized by two parameters: i) f, number of arms, i.e. bonds outcoming from each (except the terminating) segment; ii) M, the number of generations, i.e. number of segments contained in a chain connecting the central and terminating segment minus one. Dendrimers with f arms and M generations will be abbreviated by $D(f, M)$.

Each dendrimer contains a central a segment, which is by definition segment of generation 0. Segments of the

*Electronic address: a.malijevsky@imperial.ac.uk

ith generation are connected to the central segment by a chain of $i+1$ segments. The number of segments of ith generation is $g_i = f\cdot(f-1)^{i-1}$, $i \geq 1$ and the total number of segments is $N = f\frac{1-(f-1)^M}{2-f}+1$.

Segment positions are labeled by two indexes; the subscript, $i = 0..M$, specifying the generation, and the superscript, $j = 1..g(i)$, specifying the position in a given generation. The latter can be set in a clockwise order (in a two-dimensional projection) such that segments $\mathbf{r}_i^1,\ldots,\mathbf{r}_i^{f-1}$ are connected to the segment $\mathbf{r}_{i-1}^1$. Position of a whole dendrimer can be expressed by a vector $\mathbf{R} = \prod_{i=0}^{M}\prod_{j=1}^{g(i)}\mathbf{r}_i^j$.

The model under interest will be represented by tangentially connected hard spheres of diameter σ, each interacting via potential ψ with an external field. The grand potential functional of such a system can be expressed as [14]

$$\beta\Omega[\rho_N(\mathbf{R})] = \beta F_{\rm id}[\rho_N(\mathbf{R})]+\beta F_{\rm ex}+\int[\Psi(\mathbf{R})-\mu]\rho_N(\mathbf{R})\mathrm{d}\mathbf{R}\,, \tag{1}$$

where

$$\beta F_{\rm id} = \int \mathrm{d}\mathbf{R}\rho_N(\mathbf{R})[\log\rho_N(\mathbf{R})-1]+\beta\int\mathrm{d}\mathbf{R}\rho_N(\mathbf{R})V_b(\mathbf{R}) \tag{2}$$

is the contribution corresponding to the system of ideal chains that interact only through bounding potential, $V_b(\mathbf{R})$, and the excess part that takes into account correlations between nonbonded segments

$$\beta F_{\rm ex} = \int \mathrm{d}\mathbf{r}\left\{\Phi^{\rm hs}[n_\alpha(\mathbf{r})]+\Phi^{\rm c}[n_\alpha(\mathbf{r})]\right\} \tag{3}$$

is split into the hard-sphere contribution $\Phi^{\rm hs}$ and the contribution due to the chain connectivity $\Phi^{\rm c}$.

$\rho_N(\mathbf{R})$ is the dendrimer density and $\Psi(\mathbf{R}) = \sum_{i=0}^{M}\sum_{j=1}^{g(i)}\psi(\mathbf{r}_i^j)$. Further, $V_b(\mathbf{R})$ is a sum of bounding potentials between the neighboring segments creating the dendrimer structure,

$$\exp[-\beta V_b(\mathbf{R})] = \prod_{i=0}^{M-1}\prod_{j=1}^{g(i)}\prod_{k=-\delta_{i0}}^{f-2}\frac{\delta(|\mathbf{r}_i^j-\mathbf{r}_{i+1}^{j(f-1)-k}|-\sigma)}{4\pi\sigma^2}\,. \tag{4}$$

Free energy densities $\Phi^{\rm hs}[n_\alpha(\mathbf{r})]$ and $\Phi^{\rm c}[n_\alpha(\mathbf{r})]$ are functions of four scalar and two vector weighted densities $\{n_\alpha(\mathbf{r})\}$ [14, 17]. For the hard-sphere contribution, $\Phi^{\rm hs}[n_\alpha(\mathbf{r})]$, the so-called White-Bear approach (or modified FMT) have been used, see Refs. [14, 24] for the explicit formulae.

The free energy density due to indirect chain connectivity, $\Phi^{\rm c}[n_\alpha(\mathbf{r})]$, was obtained as a generalization of Wertheim's first-order perturbation theory for a bulk fluid [15, 16] for inhomogeneous systems within the nonlocal DF framework [14]

$$\Phi^{\rm c}[n_\alpha(\mathbf{r})] = \frac{1-N}{N}n_0\zeta\ln[g_{\rm HS}(\sigma,\{n_\alpha\})]\,, \tag{5}$$

where $\zeta = 1-\mathbf{n}_2\cdot\mathbf{n}_2/(n_2)^2$, and the contact value of the hard-sphere pair correlation function, $g_{\rm HS}(\sigma,\{n_\alpha\})$, is obtained from the Carnahan-Starling equation of state. The important feature of this approach is that the problem is formulated on the level of average segment density, $\rho(\mathbf{r})$, which is related to the density of a whole dendrimer $\rho_N(\mathbf{R})$ via

$$\rho(\mathbf{r}) = \sum_{i=0}^{M}\sum_{j=1}^{g(i)}\rho_i^j(\mathbf{r}) = \sum_{i=0}^{M}\sum_{j=1}^{g(i)}\int\mathrm{d}\mathbf{R}\delta(\mathbf{r}-\mathbf{r}_i^j)\rho_N(\mathbf{R}) \tag{6}$$

where $\rho_i^j(\mathbf{r})$ is the density distribution of an individual segment.

A minimization of the grand potential functional with respect to the density distributions gives rise to a set of the following Euler-Lagrange equations:

$$\rho_i^j(\mathbf{r}) = \exp(\beta\mu)\int\mathrm{d}\mathbf{R}\delta\left(\mathbf{r}-\mathbf{r}_i^j\right)\exp\left[-\beta V_b(\mathbf{R})\right]\gamma(\mathbf{r}) \tag{7}$$

and

$$\rho(\mathbf{r}) = \exp(\beta\mu)\int\mathrm{d}\mathbf{R}\sum_{i=0}^{M}\sum_{j=1}^{g(i)}\delta\left(\mathbf{r}-\mathbf{r}_i^j\right)\exp\left[-\beta V_b(\mathbf{R})\right]\gamma(\mathbf{r})\,. \tag{8}$$

Due to symmetry, $\rho_i^j(\mathbf{r})$ depends on its generation number only, so that the upper index will be omitted. Function $\gamma(\mathbf{r})$ is defined as

$$\gamma(\mathbf{r}) = \exp\left\{-\beta\prod_{i=0}^{M}\prod_{j=1}^{g(i)}\left[\frac{\delta F_{\rm ex}}{\delta\rho_i^j(\mathbf{r})}+\psi\left(\mathbf{r}_i^j\right)\right]\right\}\,. \tag{9}$$

Specifically, the segment density distributions have been calculated for hard-sphere dendrimers confined by two plane hard walls placed a distance H apart, i.e. the external field interacts with each segment with a potential

$$\psi(z) = \begin{cases}\infty & z<\sigma/2 \text{ or } z>H-\sigma/2\\ 0 & \text{otherwise}\end{cases} \tag{10}$$

For this system $\rho_i^j(\mathbf{r}) = \rho_i^j(z)$, and the the Euler-Lagrange equations have much simpler forms:

$$\rho_0(z) = \exp(\beta\mu)\gamma(z)(G_M(z))^f \tag{11}$$

and

$$\rho_i(z) = \exp(\beta\mu)\gamma(z)(G_{M-i}(z))^{f-1}\tilde{G}_i(z)\;i\geq 1\,. \tag{12}$$

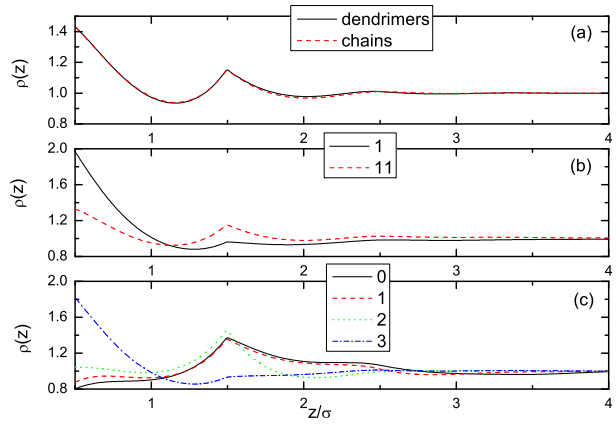

FIG. 1: (a) The average segment density of third generation dendrimers, $D(3,3)$, and linear chains, of $N = 22$ segments. (b) Segment density profiles of the first and eleventh segments of linear chains, of $N = 22$ segments. (c) Segment density profiles of the zeroth, first, second, and third generations of the dendrimer $D(3,3)$. The bulk segment density is $\rho_b^* = 0.5$. The hard walls are separated by $H = 10\sigma$.

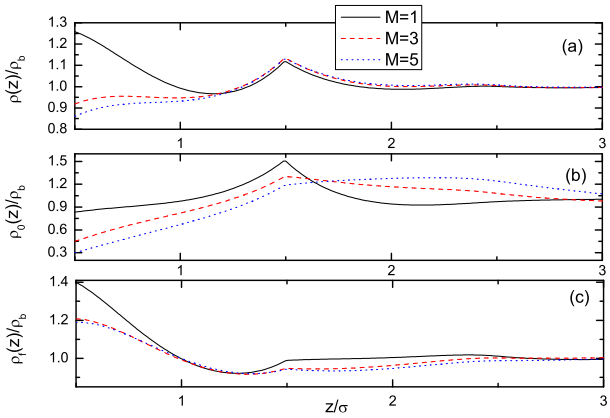

FIG. 2: Density profiles of dendrimers $D(3,1)$, $D(3,3)$, and $D(3,5)$ for $H = 10\sigma$ and $\rho_b^* = 0.4$. (a) The average segment density; (b) Segment density of cores (segments of zeroth generation); (c) Segment density of terminal segments.

The functions $G_i(z)$ and $\tilde{G}_i(z)$ are defined by the following recurrence relations

$$G_i(z) = \int \mathrm{d}z' \gamma(z') (G_{i-1}(z'))^{f-1} \frac{\theta(\sigma - |z - z'|)}{2\sigma} \quad i \geq 1 \tag{13}$$

and

$$\tilde{G}_i(z) = \int \mathrm{d}z' \gamma(z') \tilde{G}_{i-1}(z') (G_{M-i+1}(z'))^{f-2} \frac{\theta(\sigma - |z - z'|)}{2\sigma} \quad i \geq 2 \tag{14}$$

with $G_0(z) = 1$ and

$$\tilde{G}_1(z) = \int \mathrm{d}z' \gamma(z') (G_M(z'))^{f-1} \frac{\theta(\sigma - |z - z'|)}{2\sigma}.$$

In Fig. 1 comparison of the density profiles for third generation $D(3,3)$ with the profiles of linear chain polymers comprising the same number of tangent segments, i.e. $N = 22$, is shown. The latter are obtained from the theory of Yu and Wu [14]. The calculations have been performed for an average bulk segment density of $\rho_b^* = \rho_b \sigma^3 = 0.5$. It is evident from the upper panel that the average segment densities of dendrimers and chains are very similar for such a density. Both profiles exhibit oscillation characteristic with adsorption on the wall. The system is thus in the regime where the structure of the fluid is dominated by excluded volume effects. In such a case the specific architecture of the molecules plays a less important role and the system as a whole behaves like a hard-sphere system. It is interesting to note the identical contact densities, $\rho(\sigma/2)$, which reflects an equality of bulk pressures of both systems according to the sum rule [25]. This is because the systems are treated in the TPT1 approximation where only number of bonds (not their topology), which are same for both models, are taken into account.

Although the average segment densities are nearly identical, there are large differences in the densities of individual segments. In Fig. 1b the density profiles of the terminal and middle segments of chains are plotted. They both exhibit qualitatively similar behaviour to the average segment density, with higher value of contact density for the terminal segment. This is because of a smaller loss of orientational entropy if the terminal rather than the middle segment is at the contact with the wall in the case of chains and because of excluded volume interactions from the outer segments in the case of dendrimers. The density profiles of the remaining segments smoothly interpolate between these two curves. The behaviour observed for dendrimers is very different, see Fig. 1c. In this case only the terminal segments are in a regime where excluded volume effect dominates whereas all other segments exhibit surface depletion. Clearly, the terminal segments can be adsorb on to the wall more easily then those of lower generations. Because the number of segments of the highest generation is more than half of the total number of segments the adsorption for the average segment density persists. In all cases a cusp in the density profiles a distance σ from the sphere-wall contact position which reflects harshness of the fluid-fluid and the fluid-wall interaction.

The impact of the generation number on a structure of the fluid is examined in Fig 2. The calculations are carried out for $D(3,1)$, $D(3,3)$, and $D(3,5)$ for a bulk density $\rho_b^* = 0.4$. Now significant differences for different architectures are apparent in the average density profiles, see Fig. 2a. We observe a transition from surface adsorption for $D(3,1)$ (the simplest star polymer) to depletion for $D(3,3)$ and $D(3,5)$. Interestingly for the third generation dendrimer $D(3,3)$ the effect of deple-

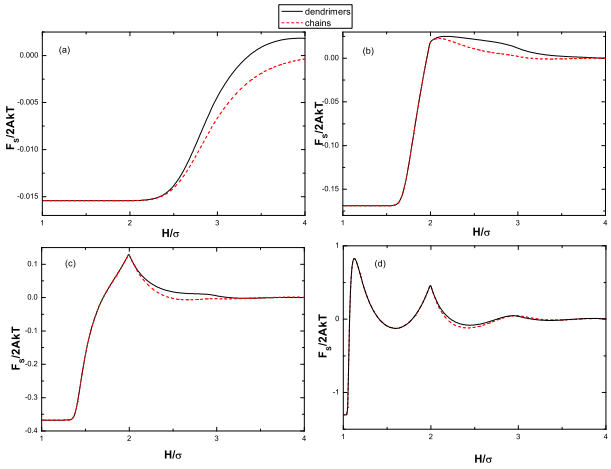

FIG. 3: Solvation forces between two hard walls separated by third generation dendrimers $D(3,3)$ (continuous curves) and linear chains of $N = 22$ segments, (dashed curves). The average bulk segment densities are (a) $\rho_b = 0.1$, (b) $\rho_b = 0.3$, (c) $\rho_b = 0.4$, (d) $\rho_b = 0.6$

tion and adsorption almost compensate each other. The density profiles of the zeroth generation segments (the cores) and the terminal segment are compared in Figs. 2b and 2c, respectively. Whereas in all three cases the zeroth segments exhibit depletion, adsorption is always found for terminal segments. Larger differences are apparent for the central segments, particularly in the slopes of the profiles beyond the cusps which change from negative to positive with increasing M, being close to zero for $D(3,3)$.

In a final analysis the solvation forces between the two hard walls are calculated for two models, $D(3,3)$ and the equivalent linear chains of $N = 22$ tangent segments. According to the sum rule [25], the solvation force F_S per unit area A is related to the average contact density through $F_S/(2Ak_bT) = \rho(0) - \rho_\infty(0)$, where $\rho_\infty(0)$ is the average contact density for infinite separation. In Figure 3 the four regimes corresponding to bulk densities $\rho_b = 0.1, 0.3, 0.4$, and 0.6 that the solvation forces can obey for the two models under consideration are presented. At the lowest density, Fig. 3a, the depletion forces dominate, so that the solvation force is attractive for small separations. At larger separations the attraction decays monotonically to zero in the case of linear hard-sphere chains whereas for dendrimers F_S first changes sign and eventually converges to zero. For intermediate densities, Fig. 3b and Fig. 3c, both solvation force profiles exhibit a maximum which is smooth for $\rho_b = 0.3$ but which for the higher density of $\rho_b = 0.4$ becomes a cusp. At the highest density of $\rho_b = 0.6$, Fig. 3d, the specific topology of molecules becomes irrelevant and both solvation force profiles have very similar oscillatory characteristics of hard-sphere systems.

In this work a density functional theory for a primitive model of dendrimers is proposed. A compact recursive formulae is derived involving both intra- and intermolecular forces taking the form of simple integrals which greatly facilitates the numerical calculations. This is the first step in a theoretical treatment of more realistic models of dendrimers for which the theory can be straightforwardly extended by using of a perturbation technique. It will enable to study various interesting problems; for instance, one of the controversy is whether dendrimers of higher generations adopt a membrane-like surface [26] or exhibit rather homogeneous segmental density due to back-folding effects [27]. Behavior of dendrimers in concentrated solutions is also of an interest. The quantitative agreement of DF theory for star polymers (the simplest case of dendrimers) derived on a similar basis [20] with Monte-Carlo data gives one confidence that the theory developed in the present work provides an accurate representation of dendrimeric systems. However, only more detailed numerical tests for corresponding models will reveal to what extent the proposed theory for dendrimers is appropriate, a matter of current research.

[1] W. Wehner G. E. Buhleier, and F. Vögtle, Synthesis **155**, 155 (1978).
[2] B. Klajnert and M. Bryszewska, Acta Biochim. Pol. **48**, 199 (2001).
[3] J. F. G. A. Jansen E. M. M. de Brabender van den Berg, and E. W. Meijer, Science **266**, 1226 (1994).
[4] N. N. Hoover B. J. Auten, and B. D. Chandler, J. Phys. Chem. B **110**, 8606 (2006).
[5] Q. S. Hu V. Pugh, M. Sabat, and L. Pu, J. Org. Chem. **64**, 7528 (1999).
[6] O. Haba K. Haga, M. Ueda, O. Morikawa, and H. Konishi, Chem. Mater. **11**, 437 (1999).
[7] K. H. Boubbou and T. H. Ghaddar, Langmuir **21**, 8844 (2005).
[8] P. J. Flory, J. Chem. Phys. **17**, 1347 (1949).
[9] A. A. Louis, P. G. Bolhuis, J. P. Hansen, and E. J. Meijer, Phys. Rev. Lett. **85**, 2522 (2000).
[10] C. N. Likos, Phys. Rep. **348**, 247 (2001).
[11] I. O. Götze, A. J. Archer, and C. N. Likos, J. Chem. Phys. **124**, 084901 (2006).
[12] C. E. Woodward, J. Chem. Phys. **94**, 3138 (1991).
[13] J. Forsman, C. E. Woodward, and B. C. Freasier, J. Chem. Phys. **117**, 1915 (2002).
[14] Y. X. Yu and J. Z. Wu, J. Chem. Phys. **117**, 2368 (2002).
[15] M. S. Wertheim, J. Chem. Phys. **87**, 7323 (1987).
[16] W. G. Chapman, G. Jackson, and K. E. Gubbins, Molec. Phys. **65**, 1057 (1988).
[17] Y. Rosenfeld, Phys. Rev. Lett. **63**, 980 (1989).
[18] D. P. Cao and J. Z. Wu, J. Chem. Phys. **117**, 2368 (2002).
[19] D. P. Cao and J. Z. Wu, Macromolecules **38**, 971 (2005).
[20] Al. Malijevský, P. Bryk, and S. Sokolowski, Phys. Rev. E **72**, 032801 (2005).
[21] C. E. Woodward and J. Forsman, Phys. Rev. Lett. **100**, 098301 (2008).
[22] O. Pizio, A. Patrykiejew, and S. Sokolowski, J. Phys.

Chem. C **111**, 15743 (2007).
[23] L. Cheng and D. P. Cao J. Phys. Chem. B **111**, 10775 (2007).
[24] R. Roth, R. Evans, A. Lang, and G. Kahl, J. Phys.: Condens. Matter **13**, 12063 (2002).
[25] J.R. Henderson, in *Fundamentals of Inhomogeneous Fluids,* edited by D. Henderson (Dekker, New York, 1992)
[26] G. Caminati N. J. Turro, and D. A. Tomalia, J. Am. Chem. Soc. **122**, 8515 (1990).
[27] C. N. Likos M. Schmidt, H. Löwen, M. Ballauff, D. Pötschke, and P. Lindner, Macromolecules **34**, 2914 (2001).